P O L S K A   A K A D E M I A   N A U K

INSTYTUT MASZYN PRZEPŁYWOWYCH

PRACE INSTYTUTU MASZYN PRZEPŁYWOWYCH

TRANSACTIONS OF THE INSTITUTE OF FLUID-FLOW MACHINERY

88

WARSZAWA – POZNAŃ 1985

P A Ń S T W O W E   W Y D A W N I C T W O   N A U K O W E

PRACE INSTYTUTU MASZYN PRZEPŁYWOWYCH

poświęcone są publikacjom naukowym z zakresu teorii i badań doświadczalnych w dziedzinie mechaniki i termodynamiki przepływów, ze szczególnym uwzględnieniem problematyki maszyn przepływowych

*

THE TRANSACTIONS OF THE INSTITUTE OF FLUID-FLOW MACHINERY

exist for the publication of theoretical and experimental investigations of all aspects of the mechanics and thermodynamics of fluid-flow with special reference to fluid-flow machinery

---

REDAKCJA – EDITORIAL OFFICE

Instytut Maszyn Przepływowych PAN
ul. Gen. Józefa Fiszera 14, 80-952 Gdańsk, skr. pocztowa 621, tel. 41-12-71

Printed in Poland

ISBN 83-01-07020-X
ISSN 0079-3205

PAŃSTWOWE WYDAWNICTWO NAUKOWE – ODDZIAŁ W POZNANIU

Nakład 340+90 egz. Ark. wyd. 13. Ark. druk. 10,875. Papier druk. sat. kl. V, 70 g. 70×100 cm. Oddano do składania 3 I 1985 r. Podpisano do druku 5 XI 1985 r. Druk ukończono w listopadzie 1985 r. Zam. nr 240/107. S-7/712. Cena zł 220,–

DRUKARNIA UNIWERSYTETU IM. ADAMA MICKIEWICZA W POZNANIU

PRACE INSTYTUTU MASZYN PRZEPŁYWOWYCH
1985 Zeszyt 88

XU TINGXIANG

Xi'an – Liverpool*

An Experiment Aimed at Demonstrating the Validity of the Free Energy Criterion Governing the Liquid Film Breakdown**

The criterion of the minimum free energy has been proved valid for the liquid film breakdown on a horizontal surface. The experiments were carried out on some glass surfaces on which the films were formed and their breakdown took place. The breakdown resulted in a free energy loss which could be related to the mass of the film. Taking this into account, an amended equation governing the film breakdown has been presented.

Nomenclature

A – area, LG interface area,
C – specific heat,
D – specific dimension of drop or ring,
E – energy,
F_1, F_2, F_3 – functions,
G – centre of gravity,
g – gravitational constant,
H – height or thickness,
i – order of designation of liquid fragment,
M – mass,
n – number of liquid fragments,
Q – free energy loss,
R – radius of circle,
U – specific bound energy,
V – liquid volume,
ρ – liquid density,
θ – contact angle,
σ – surface tension,
ξ – loss coefficient,
Δ – change in ...,

Dimensionless quantities

$\bar{H}$ – height,
Ae – area,
He – energy ratio.

Subscripts

a – air, vapour or gas,
l – liquid,
1 – initial, before film breakdown,
2 – final, after film breakdown,
D – drop,
R – ring,
F – free
P – liquid component parts after breakdown,
T – total,
C – liquid film,
Q – interface, liquid fragment/solid surface,
S – system,

---

* Department of Power Machinery Engineering, Xi'an Jiaotong University, Xi'an, China; Research Fellow, Department of Mechanical Engineering, University of Liverpool, England.

** This paper was presented at the Colloquium EUROMECH 162 organized by the Institute of Fluid-Flow Machinery, Polish Academy of Sciences and the Technical University Karlsruhe in 1982.

g – to centre of gravity,
M – refers to inner diameter of Ring,
E – refers to outer diameter of Ring,
V – interface, gas/solid surface,
min – minimum,
cal – calculation,
mea – measurement,
LG – liquid–gas,
SG – solid–gas,
LS – liquid–solid.

1. Introduction

Liquid film breakdown has been studied by a number of people [1–6]. Several criteria of liquid film breakdown have been established. The criterion of minimum free energy is one well-known example. According to this criterion a liquid film which has a minimum stable thickness will perforate because if it remained as a film its free energy would exceed the value of the aggregate free energy contained in both the fragments and new gas/solid interface.

Rupture of the film is spontaneous. It is irreversible, it incurs an entropy increase and involves the dissipation of energy as heat.

In our experiments the phenomena of free energy loss were observed and revealed. Experiments were done on some glass surfaces on which the films were formed and their breakdown took place. Some readings, which are necessary for determining the free energy of both the films just at breakdown and the liquid components after breakdown, were taken for comparison of these free energies*).

2. Preparation of the test surfaces

Figure 1a shows some test surfaces of glass which were treated by using the special technique of grinding. The following capillary conditions must be met concurrently by the test surface at the instant of film breakdown:

(a) All liquid film must migrate to the wettable surfaces.

(b) The wettable surfaces must be completely covered by liquid.

(c) The geometry of the liquid components must permit the calculation of liquid/gas surface area and of the location of the centre of gravity of the masses.

We spent many weeks attempting to fulfil these deceptively simple conditions. Block materials tried were glass, steel and PTFE. Glass was the final choice. The working surface was ground with silicon carbide powder of average grain size 9 μm and size 3–19 μm, to obtain a fine matt surface. The surface was then masked with adhesive paper exposing only the surfaces which were to be non-wetting. These surfaces were treated with PTFE spray. The masking paper was finally removed after the non-wettable surfaces had been gently polished with paper tissue.

About 30 combinations of block material, geometric shapes and dispositions and surface treatment, were tried with limited success. Typical problems were ruptures in migra-

*) The experimental results presented in this paper have been used in the paper entitled *Free Energy Loss during the Breakdown of Liquid Film* by D. J. Ryley and Xu Tingxiang for the „International Journal of Heat and Mass Transfer".

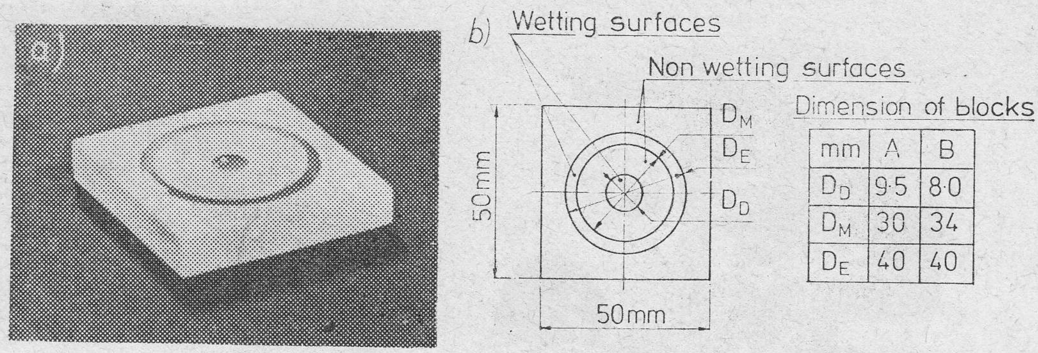

Fig. 1. Test surface; a) Photograph b) Size (thickness = 9.2 mm)

ting liquid which left residues on the non-wetting area suggesting a limit to the distance water would travel while remaining intact; also the excessive provision of wettable area which is only partially filled.

Two successful test blocks *A* and *B* (Fig. 1) were studied. Their respective dimensions are given in Fig. 1b. There may be other geometries and methods of preparation which are also adequate.

3. Experimental method

The experimental apparatus is shown in Fig. 2.

The test block with the surface fully prepared as described above, rests upon an adjustable surface carefully levelled to the horizontal. A liquid film is formed using a water syringe to cover the entire area within the diameter D_E (Fig. 1b). The film is then made progressively thinner by the slow withdrawal of liquid and its diminishing thickness is closely monitored by the micrometer microscope, magnification 35, in order to obtain the thickness at breakdown. Immediately after breakdown the respective maximum heights of the drop and of the ring are measured. Liquid weights are forthwith determined with a high precision balance by weighing the wet block, then removing one liquid component with absorbent tissue and reweighing. The weight of the dry block is known.

To ensure no significant evaporation of drop or ring occurred during measurements, observations were made of the time rates of evaporation. Evaporation during measurements was found to be negligible.

To determine the contact angles of the liquid on the glass surfaces, the photography in the plane of the prepared surface were used. The camera and lighting were arranged to show the required angle in silhouette enabling the direct measurement of the angle between the base and the tangent to the triple point. To photograph drop contact angles it was necessary first to remove the ring.

After all readings were taken, the free energy of both film and components of liquid can be calculated mathematically.

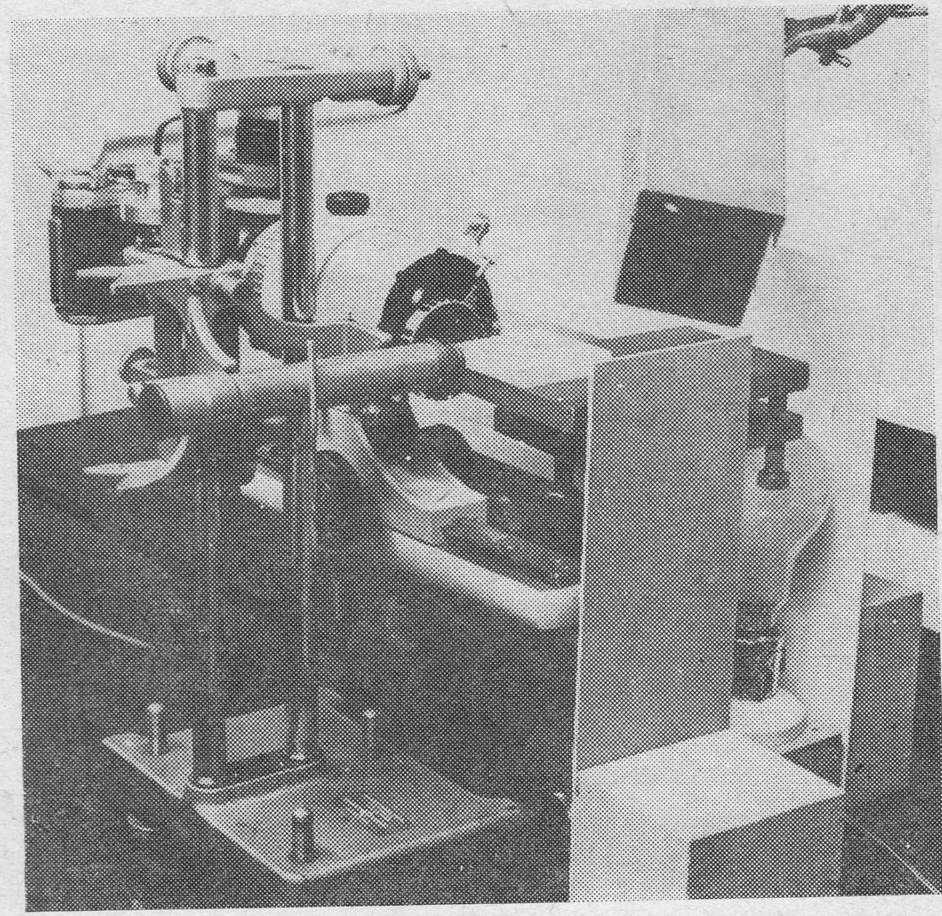

Fig. 2. Experimental apparatus

4. Free energy of the liquid film

Consider a liquid film of uniform thickness H_C (Fig. 3a) resting on a horizontal surface within a closed adiabatic boundary of arbitrary shape but drawn for convenience as a cylinder with a vertical axis. The film rests upon the lower surface. The space above the film is filled with gas (air) which does not interact with the liquid. The film is taken to be on the point of breakdown and the total energy within the system is:

$$\begin{aligned} E_{S1} &= (\text{bound energy}+\text{free energy}) \text{ in gas} \\ &\quad +(\text{bound energy}+\text{free energy}) \text{ in liquid} \\ &= [M_{a1} U_{a1} + (M_{a1} g H_{ga1} + A_{a1} \sigma_{SG})] \\ &\quad + [M_{l1} U_{l1} + (M_{l1} g H g_{l1} + A_C \sigma_{LG} + A_C \sigma_{LS})]. \end{aligned} \tag{1}$$

If

$$E_{FC1} = M_{l1} g H_{gl1} + A_C \sigma_{LG} + A_C \sigma_{LS}, \tag{2}$$

where E_{FC1} is the free energy of the film; then equation (1) can be written

$$E_{S1}=[M_{a1}\,U_{a1}+(M_{a1}\,gH_{ga1}+A_{a1}\,\sigma_{SG})]+M_{l1}\,U_{l1}+E_{FC1}\,. \tag{3}$$

The original liquid mass is

$$M_{l1}=A_C\,H_C\,\rho$$

and if the height of its centre of gravity is

$$H_{gl1}=\frac{H_C}{2}$$

equation (2) can be written as

$$E_{FC1}=A_C\,\sigma_{LG}\left(1+\frac{\sigma g H_C^2}{2\sigma_{LG}}\right)+A_C\,\sigma_{LS}\,. \tag{4}$$

Defining

$$He=\frac{\rho g H_C^2}{2\sigma_{LG}}, \tag{5}$$

where He is the ratio of the potential energy of the liquid film to its surface energy in the liquid/gas interface, equation (4) becomes

$$E_{FC1}=A_C\,\sigma_{LG}(1+He)+A_C\,\sigma_{LS} \tag{6}$$

in which the term $A_C\sigma_{LS}$ is constant for a given temperature, which fixes the magnitude

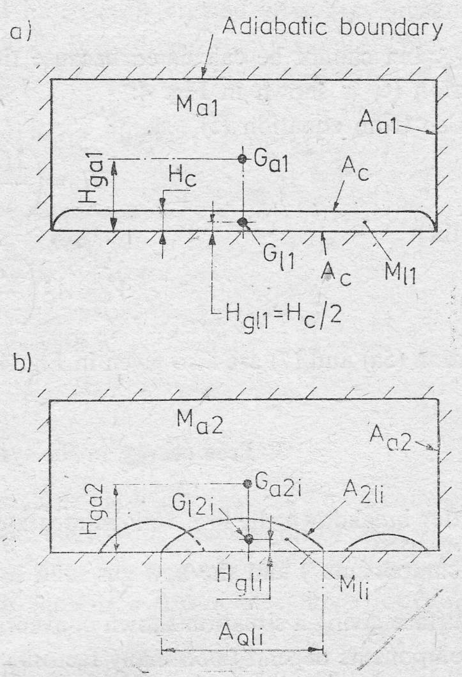

Fig. 3. Adiabatic chamber defining thermodynamic system; a) Liquid film intact just before fracture, b) Sessile liquid components following fracture

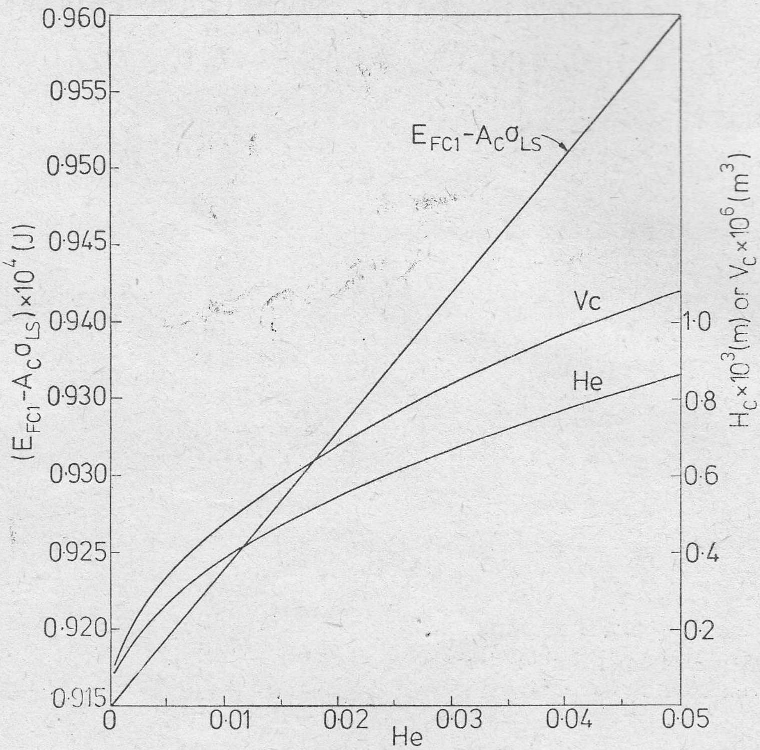

Fig. 4. Variation of free energy, thickness and volume of liquid film with *He*
$A_C=1256.6$ mm² ($Ae=168.9$)

of σ_{LS}, but cannot be calculated because the magnitude of σ_{LS} is unknown. A plot of equation (6) is shown in Fig. 4:

Also from equation (5)

$$H_C=\left(\frac{2He\sigma_{LG}}{\rho g}\right)^{\frac{1}{2}} \tag{5a}$$

and then

$$V_C=A_C\left(\frac{2He\sigma_{LG}}{\rho g}\right)^{\frac{1}{2}}. \tag{7}$$

Equation (5a) and (7) are also given in Fig. 4 diagrammatically.

5. Free energy in the system after film breakdown

After breakdown the film will disintegrate into a number of discrete liquid fragments (or "components") and the new gas/solid interface ($A_C-\sum_1^n A_{Qi1}$) will be created on the test surface giving a situation shown conventionally in Fig. 3b. The shape and number of the components depend upon many factors such as the texture of the surface, the nature of the liquid, the local variation in wettability, the distance the liquid is capable of moving along the surface and so on. The total energy within the system after breakdown is the aggregate of the individual values of bound and free energy and is given by

$$E_{S2}=[M_{a2}U_{a2}+(M_{a2}gH_{ga2}+A_{a2}\sigma_{SG})]$$
$$+[M_{l2}U_{l2}+(\sum_1^n M_{li}gH_{gli}+\sum_1^n A_{Vli}\sigma_{LG})$$
$$+\sum_1^n A_{Qli}\sigma_{LS}+(A_C-A_{Qli})\sigma_{SG}]. \quad (8)$$

The free energy of the components is given by

$$E_{FP}=\sum_1^n M_{li}gH_{gli}+\sum_1^n A_{Vli}\sigma_{LG}+\sum_1^n A_{Qli}\sigma_{LS} \quad (9)$$

and the total free energy within the system is then given by

$$E_{FT2}=E_{FP}+(A_C-\sum_1^n A_{Qli})\sigma_{SG}. \quad (10)$$

Hence equation (8) can also be given by

$$E_{S2}=[M_{a2}U_{a2}+(M_{a2}gH_{ga2}+A_{a2}\sigma_{SG})]+M_{l2}U_{l2}+E_{FT2}. \quad (8a$$

The formal approach followed thus far requires the recognition in both equations (1) and (8) of all the energy quantities associated with both the gas and the liquid both before and after breakdown. The original gas-wetted area on the walls and ceiling of the system remains unchanged. But additional gas/solid interface is created after film breakdown. To simplify understanding we assume that after breakdown a single liquid component remains resting on a reduced base. In this case, equation (9) will reduce to

$$E_{FP}=M_{l2}gH_{gl2}+A_{Vl2}\sigma_{LG}+A_{Ql2}\sigma_{LS} \quad (9a)$$

and equation (10) now reduces to

$$E_{FT2}=E_{FP}+(A_C-A_{Ql2})\sigma_{SG}. \quad (10a$$

Considering Young's equation

$$\sigma_{SG}-\sigma_{LS}=\sigma_{LG}\cos\theta \quad (11)$$

and equation (9a), equation (10a) will be

$$E_{FT2}=M_{l2}gH_{gl2}+A_{Vl2}\sigma_{LG}+(A_C-A_{Ql2})\sigma_{LG}\cos\theta+A_C\sigma_{LS}. \quad (10b)$$

For the experiments to be described above, it is necessary that the liquid components should have geometric or mathematical shapes permitting calculation of M_{l2}, H_{gl2} and A_{Vl2}. The most convenient bases were a circle which supported an axi-symmetric sessile drop ("drop") and an annulus which support a toroid of symmetrical*) profile

*) See also section 6.

('ring"). The first and second terms in the right han d of equation (10b) can now be given 'in the form of

$$M_{l2}\, gH_{gl2}=\rho g H_C^2 \cdot \frac{F_2}{F_1\,\bar{A}_{Ql2}} \cdot A_C$$

n which $\bar{A}_{Ql2}=A_{Ql2}/A_C$, and

$$A_{Vl2}\,\sigma_{LG}=\bar{A}_{Ql2}\,F_3\,\sigma_{LG}\cdot A_C.$$

Here F_1, F_2 and F_3 are generally functions of θ and the dimensionless height $\bar{H}=H/D$ of the drop or ring. The dimension D is interpreted as the diameter for the drop and the radical width for the annulus. F_1, F_2 and F_3 will be discussed in section 6. Therefore equation (10b) can be written as

$$E_{FT2}=A_C\,\sigma_{LG}\left[\frac{2HeF_2}{\bar{A}_{Ql2}\,F_1}+\bar{A}_{Ql2}\,F_3+(1-\bar{A}_{Ql2})\cos\theta\right]+A_C\,\sigma_{LS}. \qquad (10c)$$

If the liquid component has attained its steady state after breakdown its free energy should be at its minimum value. Hence $\bar{A}_{Ql2}$ corresponding to minimum free energy can be obtained by differentiating equation (10c) with respect to $\bar{A}_{Ql2}$, equating to zero and

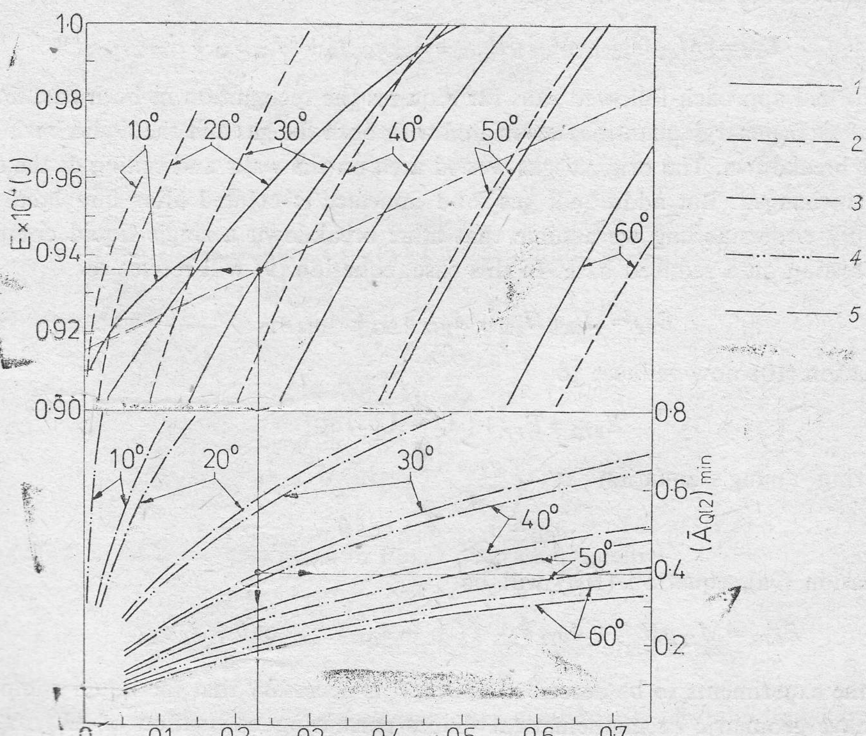

Fig. 5. Variation of free energy and area ratio for drop and ring when the profile is modelled as the segment of a circle

1 − $E=(E_{FTD})_{min}-A_C\sigma_{LS}$, 2 − $E=(E_{FTR})_{min}-A_C\sigma_{LS}$, 3 − $(\bar{A}_{QlD})_{min}$, 4 − $(A_{QlR})_{min}$, 5 − Free energy of film $E=E_{FCl}-A_C\sigma_{LS}$

solving, thus obtaining

$$(\bar{A}_{Q12})_{\min}=\left[\frac{2HeF_2}{F_1(F_3-\cos\theta)}\right]^{\frac{1}{2}}. \tag{12}$$

Substituting equation (12) into (10c) one obtains the following relation for the minimum free energy of a stable drop or ring

$$(E_{FT2})_{\min}=A_C\sigma_{LG}\left(2\left[\frac{2HeF_2(F_3-\cos\theta)}{F_1}\right]^{\frac{1}{2}}+\cos\theta\right)+A_C\sigma_{LS}. \tag{13}$$

In Fig. 5 the free energy expressed as $(E_{FT2})_{\min}-A_C\sigma_{LS}$ calculated from equation (13) is presented together with the corresponding $(\bar{A}_{Q12})_{\min}$ for both the drop and the ring when their profiles were assumed to be taken as Fig. 7a. The free energy of the original film E_{FC1} obtained from equation (4) is also shown.

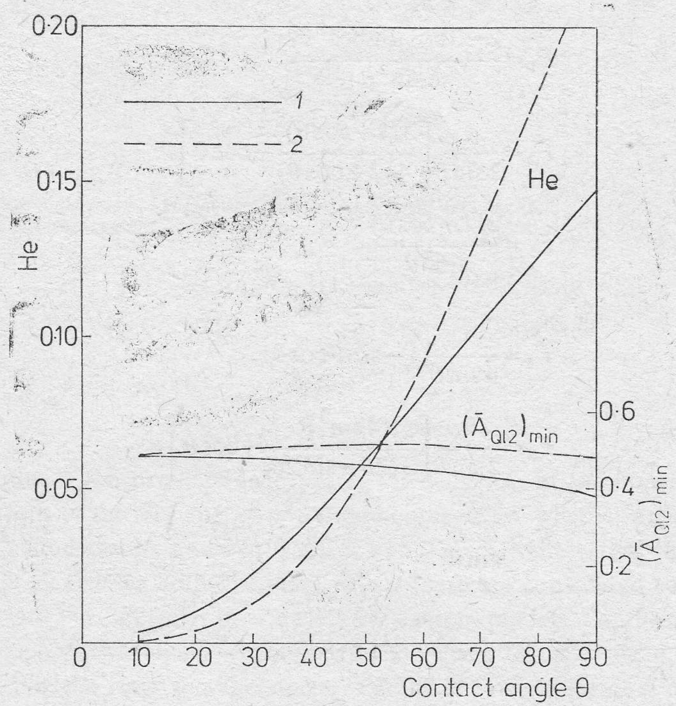

Fig. 6. Variation of He and $(A_{Q12})_{\min}$ with θ when profile is the segment of a circle
1 – Drop, *2* – Ring

Previous investigators have assumed that the free energy of the film is conserved during breakdown and is thus equal to the aggregate free energies of the liquid components and the new gas/solid interface. Thus in Fig. 5 each intersection point with the free energy curve for the film by that for a drop or a ring gives the dimensionless number He and $(\bar{A}_{Q12})_{\min}$ corresponding to each contact angle θ at the condition of breakdown. Fig. 6 shows the variation of He and $(\bar{A}_{Q12})_{\min}$ with θ for free energy conservation during film breakdown.

6. Determination of the contact angles

After determining the mathematical form of the profiles the contact angle θ can then be obtained for the drop or the ring by solving

$$V = A_{Ql2} D F_1 , \tag{14}$$

the height of the centre of gravity from

$$H_{gl} = D F_2 \tag{15}$$

and the liquid/gas interfacial area from

$$A_{Vl2} = A_{Ql2} F_3 . \tag{16}$$

In equations (14) – (16), three functions F_1, F_2 and F_3 are as follows. For profile Fig. 7a,

Drop:

$$F_1 = \frac{2 - 3\cos\theta + \cos^3\theta}{6\sin^3\theta} , \tag{17}$$

$$F_2 = \frac{1}{2\sin\theta}\left[\frac{3(1+\cos\theta)^2}{4(2+\cos\theta)} - \cos\theta\right], \tag{18}$$

$$F_3 = \frac{2(1-\cos\theta)}{\sin^2\theta} , \tag{19}$$

Ring:

$$F_1 = \frac{1}{4\sin\theta}(1 - \sin\theta\cos\theta) , \tag{17a}$$

$$F_2 = \frac{1}{2\sin\theta}\left[\frac{4\sin^3\theta}{3(2\theta - \sin 2\theta)} - \cos\theta\right], \tag{18a}$$

$$F_3 = \frac{\theta}{\sin\theta} . \tag{19a}$$

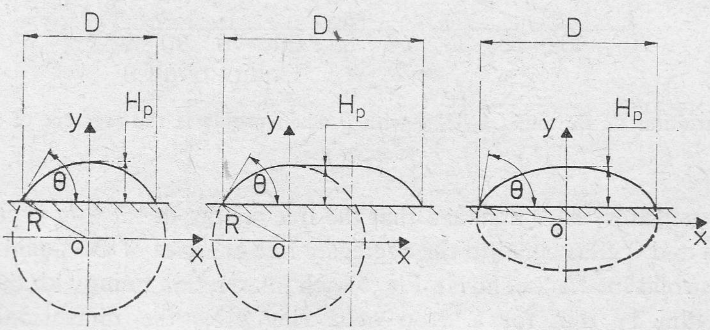

Fig. 7. Model profiles for cross section of drop or ring; a) Circular, b) Displaced circular, c) Elliptical segment

For profile Fig. 7b.

Drop: $$F_1=\frac{1}{3(1-\cos\theta)^3}(4\bar{H}^3(2-3\cos\theta+\cos^3\theta)+3\bar{H}(1-\cos\theta+$$

$$-2\bar{H}\sin\theta)^2(1-\cos\theta)+6\bar{H}^2(1-\cos\theta-2\bar{H}\sin\theta)(\theta-\cos\theta\sin\theta)), \qquad (17b)$$

$$F_2=\frac{\bar{H}}{1-\cos\theta}\left\{\frac{1}{2}\frac{\left[\begin{array}{l}6\bar{H}^2\sin^4\theta+3(1-\cos\theta-2\bar{H}\sin\theta)^2\sin\theta+\\+8\bar{H}(1-\cos\theta-2\bar{H}\sin\theta)\sin^3\theta\end{array}\right]}{\left[\begin{array}{l}4\bar{H}^2(2-3\cos\theta+\cos^3\theta)+3(1-\cos\theta-2\bar{H}\sin\theta)^2\cdot\\\cdot(1-\cos\theta)+6\bar{H}(1-\cos\theta+2\bar{H}\sin\theta)(\theta-\cos\theta\sin\theta)\end{array}\right]}-\cos\theta\right\}, \qquad (18b)$$

$$F_3=\frac{1}{(1-\cos\theta)^2}(8\bar{H}^2(1-\cos\theta)+4\bar{H}(1-\cos\theta-2\bar{H}\sin\theta)\theta+$$

$$+(1-\cos\theta-2\bar{H}\sin\theta)^2); \qquad (19b)$$

Ring:

$$F_1=\frac{\bar{H}}{(1-\cos\theta)^2}(\bar{H}(\theta-2\sin\theta+\cos\theta\sin\theta+(1-\cos\theta)^2), \qquad (17c)$$

$$F_2=\frac{\bar{H}}{1-\cos\theta}\left[\frac{1}{6}\cdot\frac{4\bar{H}\sin^3\theta+3(1-\cos\theta+2\bar{H}\sin\theta)\sin^2\theta}{\bar{H}(\theta-\sin\theta+\cos\theta\sin\theta)+(1-\cos\theta)^2}-\cos\theta\right], \qquad (18c)$$

$$F_3=1+\frac{2\bar{H}(\theta-\sin\theta)}{1-\cos\theta}. \qquad (19c)$$

The definition of the profile category and the selection of the appropriate functions permit calculations of the free energy of a liquid component, whether drop or ring.

The experimental results given in Table I and Table II show that the contact angles θ have good agreement for both drop and ring if these are considered to have the profile Fig. 7a. Fig. 7b and Fig. 7c clearly provide less satisfactory models. For the case Fig. 7a, Fig. 8 gives a comparison of the calculated and measured values. The agreement is generally close for the drops. For the ring, the agreement is good at low values of θ but worsens progressively with increasing values of θ. This occurs because the ring profile is not quite symmetrical about its centre causing an increase in θ on the inside and a decrease in θ on the outside. The asymmetry arises from an inward component of surface tension. It is not possible to employ silhouette photography to determine θ on the inside of the ring, but it is reasonable to suppose that its value would be greater than that calculated and present an error trend similar to that shown on Fig. 8 and defining a mean between inside and outside values in general agreement with calculated values.

The part-elliptical profile (Fig. 7c) did not give a good representation for these experiments but was used successfully by Dr. D. J. Ryley et al. [6, 7] for small sessile drops axi-symmetric about a vertical axis.

Table 1

Comparison of the contact angle of the drops, $D_D = 8.0$ mm

Type of the drops	Height H [mm]	Weight W [mg]	Contact angle: Profiles [degree] a	b	c	Experimental value [degree]
(a)	2.746	114.0	84.7	101.5	151.6	98.0
	2.110	81.0	70.6	86.6	121.9	81.0
	1.676	63.0	60.3	77.8	125.5	60.0
	1.301	50.0	51.1	72.4	137.6	51.0
	0.983	39.0	41.6	65.6	148.9	40.0
	0.809	32.0	35.0	57.6	153.1	33.0
	0.576	27.0	30.2	93.0	170.2	30.0
	0.376	21.0	23.8	—	—	24.0
	0.231	17.0	19.6	—	—	18.0
(b)	0.694	21.0	23.8	27.2	47.3	25.0
	0.723	22.0	24.9	28.5	50.3	24.0
	0.636	22.5	25.5	35.1	132.9	24.0
	0.723	22.5	25.5	29.7	59.1	24.0
	0.665	18.0	20.6	21.5	25.3	18.0
	0.549	13.0	15.0	15.9	15.9	15.0
	0.607	15.0	17.2	17.5	17.5	17.0
	0.549	13.0	15.0	15.9	15.8	16.0

(a) Liquid placed for measurement purposes, i.e. no prior film breakdown.
(b) Following film breakdown.

Table 2

Comparison of the contact angle of the rings, $D_E = 40.0$ mm, $D_M = 34.0$ mm

Type of the rings	Height H [mm]	Weight W [mg]	Contact angle: Profile [degree] a	b	c	Experimental value [degree]
(a)	1.214	355.0	83.5	92.4	108.1	67.0
	0.954	309.0	76.9	105.2	139.8	57.0
	0.694	241.0	65.3	121.8	158.1	49.0
	0.520	153.0	46.0	64.5	129.8	41.0
	0.405	116.0	36.0	50.1	124.1	30.0
	0.289	83.0	26.6	38.6	134.6	22.0
	0.173	64.0	20.6	20.2	175.7	19.0
(b)	0.462	120.0	37.2	41.6	59.6	34.0
	0.491	134.0	41.1	49.6	88.3	34.0
	0.636	170.0	50.2	56.7	79.4	40.0
	0.809	200.0	57.1	57.5	58.6	48.0
	0.462	113.0	35.3	36.5	40.4	30.0
	0.549	134.0	41.1	42.1	44.9	41.0

a) Liquid placed for measurement purposes, i.e. no prior film breakdown.
(b) Following film breakdown.

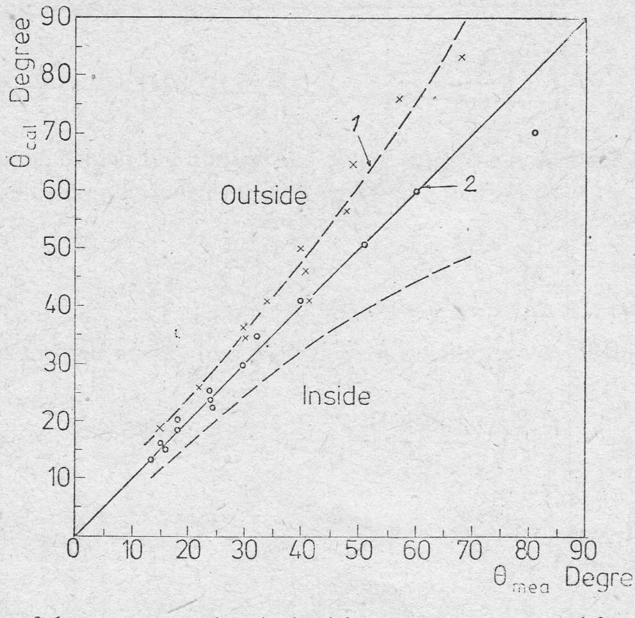

Fig. 8. Comparison of th e contact angles obtained from measurements and from calculation when th profile is modelled by a circular segment.

1—Drop, *2*—Ring

7. Free energy loss at film breakdown

Fig. 9 gives experimentally the variation of the free energy of both the film and the liquid components and new gas/solid interface with *He*. It is very clear that the free energy of film is more than that of the aggregation of both the liquid components and new gas/solid interface at the same *He*. The difference ΔE_F between them is also given in Fig. 9. It shows that there exists a free energy loss during the film breakdown and that the free energy loss increases with *He*. In fact, the breakdown process is spontaneous and therefore irreversible and accompanied by entropy production. Expenditure of energy is necessary to modify the sizes and locations of the enclosed gas and liquid. This energy is degraded into heat by viscous action and the system temperature rises. It should, in principle, be possible to assess the extent of the energy degradation.

Considering the system as a whole at film breakdown there can be no loss of energy, i.e. within the adiabatic boundary

$$E_{S1} = E_{S2}\,. \tag{20}$$

However, the gas free energy quantities are either small or unchanged. Therefore, we can have, from equations (3), (8a) and (20):

$$M_{l1}\,U_{l1} + E_{FC1} = M_{l2}\,U_{l2} + E_{FT2}\,.$$

Hence, letting

$$\Delta E_F = E_{FC1} - E_{FT2} \qquad (21$$

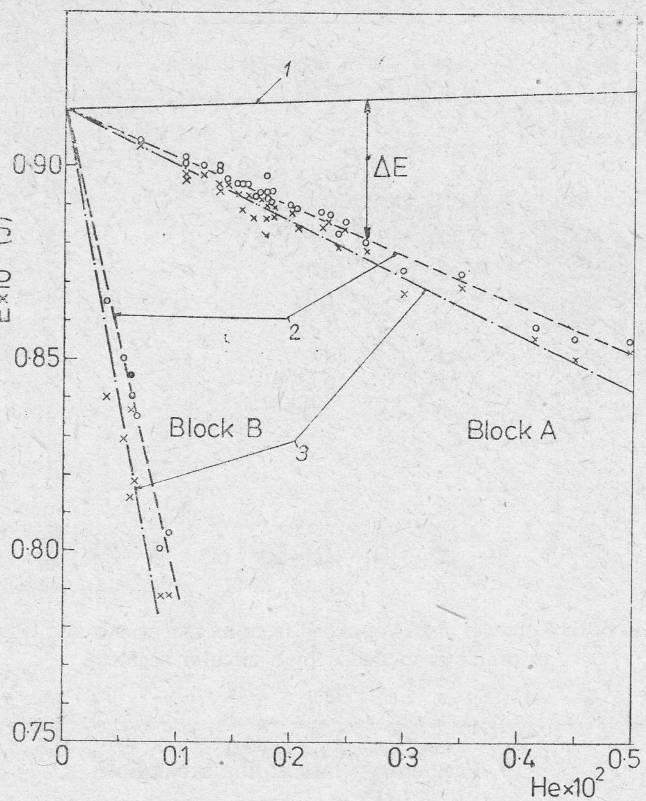

Fig. 9. Free energy loss at film breakdown with *He*

$1-E=E_{FC1}-A_C\sigma_{LS}$, $2-E=(E_{FT2})_{min}-A_C\sigma_{LS}$ for profile Fig. 7a, $3-E=(E_{FT2})_{min}-A_C\sigma_{LS}$ for profile Fig. 7b

which is defined as the free energy loss at film breakdown, then

$$\Delta E_F = M_{l2}\, U_{l2} - M_{l1}\, U_{l1}\,. \tag{22}$$

Actually, the mass of liquid is unchanged within the system, i.e.

$$M_{l1} = M_{l2} = M_l$$

then

$$\Delta E_F = M_l (U_{l2} - U_{l1})\,. \tag{22a}$$

Equation (22a) can also be written:

$$\Delta E_F = M_l \cdot C_l \cdot \Delta T, \tag{22b}$$

where C_l is the specific heat of liquid and ΔT is the temperature increase incurred by film breakdown. ΔT actually is so small that it is not possible for it to be measured in the usual way. Furthermore, in the engineering context, film breakdown does not take place with an adiabatic system, but in the "open". This is also the case for laboratory experiments and measurements must be made in that situation.

Considering equations (6) and (13):

$$\varDelta E_F = A_C \sigma_{LG} \left\{ (1+He) - 2\left[\frac{2HeF_2(F_3 - \cos\theta)}{F_1} \right]^{\frac{1}{2}} - \cos\theta \right\}. \tag{23}$$

Substituting He under which the film breaks down, free energy loss $\varDelta E_F$ can then be calculated, for difference contact angles θ, according to equation (23).

Let

$$\xi = \frac{\varDelta E_F}{E_{FC1} - A_C \sigma_{LS}} \tag{24}$$

which is defined as the free energy loss coefficient at the film breakdown and also is shown in Fig. 8.

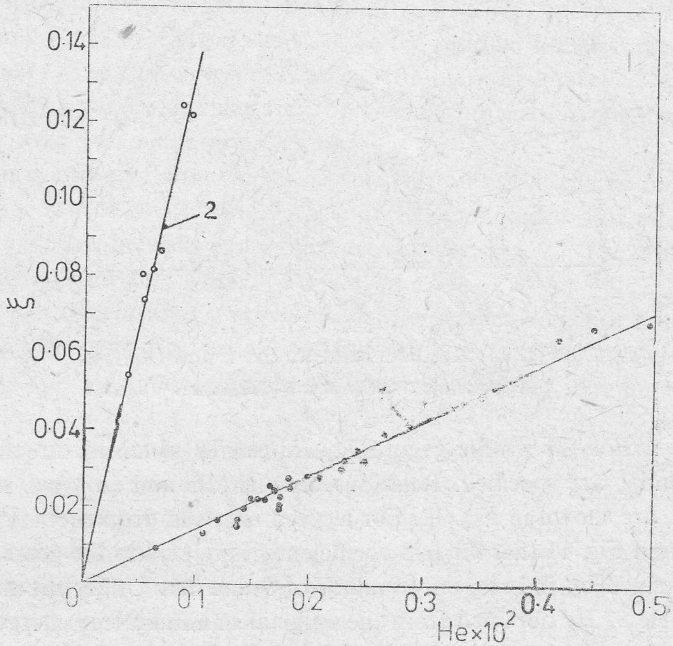

Fig. 10. Free energy loss coefficient at film breakdown and *He*

– Block A, 2 – Block P

It is clear that from equation (24)

$$E_{FC1} = E_{FT2} + \xi(E_{FC1} - A_C \sigma_{LS}), \tag{25}$$

Substituting equations (6) and (13) into equation (25) one obtains, after some manipulation:

$$(1-\xi)^2 He^2 + 2\left[(1-\xi)(1-\xi-\cos\theta) - \frac{4F_2(F_3-\cos\theta)}{F_1} \right] He + (1-\xi-\cos\theta)^2 = 0 \tag{26}$$

which can be considered as an amended criterion of minimum free energy governing liquid

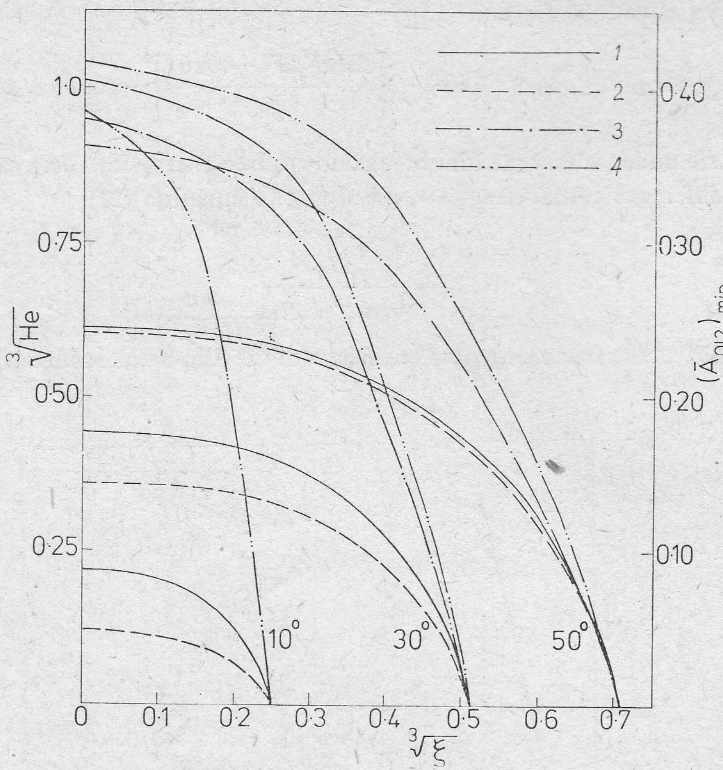

Fig. 11. Relation between *He*, ξ and $(\bar{A}_{Q12})_{\min}$

1 – *He* for drop, *2* – *He* for ring, *3* – $(\bar{A}_{Q1D})_{\min}$, *4* – $(\bar{A}_{Q1R})_{\min}$

film breakdown. For the profile Figure 7a, *He* can be obtained directly from equation (26) when θ and ξ are specified. Relations between *He* and $(\bar{A}_{Q12})_{\min}$ with ξ and θ, for profile Fig. 7a, are shown in Fig. 11. For a given ring and drop geometry it is seen from equation (26) and Fig. 11 that the loss coefficient ξ is related to the geometry of the liquid components defined by the respective values of θ and *He*. Under the same condition of the contact angle θ, *He* obtained from the original minimum free energy criterion ($\xi=0$) is larger than that obtained from the amended minimum free energy criterion ($\xi\neq 0$). It means that practical critical film thicknesses are thinner than those calculated from the original minimum free energy criterion at the same contact angle θ.

For the profile Fig. 7b, equation (26) remains valid, but reference to equations (17b), (18b) and (19b) for the drop and (17c), (18c) and (19c) for the ring shows that each equation now contains $\bar{H}=H/D$ thus introducing a further unknown and requiring an additional equation as follows:

$$He=\frac{2}{\pi}Ae\bar{A}_{Q12}^{3}F_1^2 \qquad 27)$$

for the drop, and

$$He=\frac{Ae\bar{A}_{Q12}^{2}}{2\pi}\left(1-\sqrt{1+\bar{A}_{Q12}^{2}F_1^2}\right) \qquad (28)$$

for the ring, where

$$Ae=\frac{\rho g A_C}{\sigma_{LG}} \tag{29}$$

which is directly proportional to the cube of the ratio: diameter of unbroken film/its thickness (D_C/H_C).

Combining equations (12), (26), and (27) or (28), the relations of He, ξ, $(\bar{A}_{Ql2})_{\min}$ and $\bar{H}$ can be solved for a given A_C.

8. Conclusions

This work leads to the following conclusions. For a horizontal surface:

1. It is possible to verify experimentally the validity of the free energy criterion for the breakdown of a liquid film for selected cases where the residual liquid components each have a simple geometry. The chosen test surface constraints were a circular area surrounded at some distance by a narrow annular area, both rendering wetting possible. The wider intervening annular area was made non-wetting.
2. The liquid film wetting an annulus has a cross section which can be modelled by a circular segment (Fig. 7a) for small contact angle and a small width. For a larger width, the section is a narrow plane between ends which are circular, Fig. 7b. The model (Fig. 7a) is generally used throughout this work.
3. The conditions in conclusion (2) apply also to the sessile drop. For a large contact angle and small size, the segment of an ellipse (Fig. 7c) gives a closer model.
4. There is a minimum stable film thickness at which the film has minimum free energy and breaks down.
5. During the act of breakdown there is a free energy loss in the form heat arising from the spontaneous and therefore irreversible nature of the change. The curves of loss coefficient, ξ, shown in Fig. 9, suggest that the losses increase both with the increase in non--wetting area to be crossed by the migrating liquid and also with the increase in He. The former suggests enhanced fluid friction losses in transit. The reason for the latter is not clear. Especially interesting is the linear variation of ξ with He for both cases A and B.
6. Equation (26) describing free energy loss during film breakdown can be regarded as an amended equation governing liquid film breakdown.
7. Under the condition of the same contact angle θ, He obtained from the original minimum free energy criterion ($\xi=0$) is larger than the practical value which can be obtained from the amended equation of liquid film breakdown.

Acknowledgements. The experimental work was carried out in the Wet Steam Laboratory, University of Liverpool, in 1981-82.

Enlightening and deep discussions with Dr. D. J. Ryley are most gratefully acknowledged.

I am also grateful to Mr. Eric Hughes who helped with the construction of apparatus and the experimental work.

Received by the Editor, February 1984.

References

[1] D. E. Hartley and W. Murgatroyd, *Criteria for the break-up of thin liquid layers flowing isothermally over a solid surface*. Int. J. Heat Mass Transfer, 7, 1003 (1964).

[2] W. Murgatroyd, *The role of shear and form forces in the stability of a dry path in two-phase film flow*. Int. J. Heat Mass Transfer, 8, 297 (1965).

[3] S. G. Bankoff, *Minimum thickness of a draining liquid film*. Int. J. Heat Mass Transfer, 14, 2143 (1971).

[4] J. Mikielewicz and J. R. Moszyński, *Minimum thickness of a liquid film flowing vertically down a solid surface*. Int. J. Heat Mass Transfer, 19, 771 (1976).

[5] B. H. Khoshaim, *The flow of rivulets over L. P. steam turbine guide blades*. Ph. D. Thesis, The University of Liverpool, 1975.

[6] D. J. Ryley and B. H. Khoshaim, *A new method of determining the contact angle made by a sessile drop upon a horizontal surface*. J. Coll. Interface Sci., 59, 2, April 1977, pp. 243 - 251.

[7] D. J. Ryley and M. S. B. Ismail, *The shape of sessile water drops on inclined plane surface*. Ibid, 65, 2, June 1978, pp. 394 - 396.

Doświadczalna ilustracja słuszności kryterium energii swobodnej w odniesieniu do przerwania filmu cieczowego

Streszczenie

Płaska powierzchnia poziomo leżącego bloku szkła została poddana obróbce, w wyniku której niektóre obszary można było zwilżyć wodą a inne były niezwilżalne. Utworzono kolisty obszar (zwilżalny, ,,kropla") otoczony pierścieniem (niezwilżalnym), który z kolei znajdował się wewnątrz drugiego wąskiego pierścienia (zwilżalny, ,,pierścień"). Wszystkie okręgi ograniczające te obszary były współśrodkowe.

Cały obszar objęty zewnętrznym okręgiem pokryto warstewką cieczy. Grubość warstewki zmniejszano, doprowadzając do jej perforacji i pokrycia przez wodę obszarów zwilżalnych. Mierzono wysokość i masę cieczy zarówno początkowej warstewki jak też kropli i pierścienia. Pozwoliło to na obliczenie wyjściowej energii swobodnej oraz łącznej końcowej energii swobodnej.

W opisanych warunkach zachodzi strata energii. Można ją odnieść do masy filmu cieczowego. Geometrię powstałych powierzchni można obliczać dzięki odpowiedniemu zamodelowaniu profili pierścienia i kropli krzywymi umożliwiającymi analizę. Najlepsze dopasowanie zapewniał fragment okręgu.

Na skutek początkowej straty energii swobodnej końcowa energia swobodna jest mniejsza od wyjściowej energii swobodnej, a grubość filmu na końcu przemiany jest większa od jej wartości odpowiadającej końcowej energii swobodnej. Uwzględniając stratę energii swobodnej przedstawiono skorygowane równanie opisujące przerwanie filmu cieczowego.

Экспериментальная иллюстрация правильности критерия свободной энергии по отношению к разрыву жидкостной пленки

Резюме

Плоская поверхность горизонтально расположенного стекляного блока подвергалась обработке, в результате которой некоторые зоны можно было смачивать, а другие оставались несмачиваемыми. Образована круговая зона (смачиваемая, ,,капля"), окруженная кольцом (несмачи-

ваемым), которое очередно находилось внутри второго узкого кольца (смачиваемого, ,,кольцо") Все окружности ограничивающие эти зоны, являлись концентрическими.

Вся зона охваченная внешней окружностью была покрыта пленкой жидкости. Толщину пленки постепенно уменьшалось, приводя к ее перфорации и к покрытию водой смачиваемых зон. Измерялась высота и масса жидкости, так начальной пленки как капель и кольца. Это позволило вычислить выходную свободную энергию и суммарную концевую свободную энергию.

В описанных условиях имеются потери энергии. Их можно отнести к массе жидкостной пленки. Геометрию возникших поверхностей можно определить на основе соответственного моделирования профилей кольца и капли кривыми позволяющими производить анализ. Наилучшее приспособление обеспечивал фрагмент окружности.

Вследствие наличия начальной потери свободной энергии концевая свободная энергия оказывается меньшей от выходной свободной энергии, а толщина пленки у конца превращения является большейот ее значения, отвечающего концевой свободной энергии. Учитывая потерю свободной энергии представлено прокорректированное уравнение описывающее разрыв жидкостной пленки.